Electronic Supplemental Information File

One-step preparation of bioactive enzyme/inorganic materials

*Mansi Malhotra[a], Megan K. Puglia[a], Clive L. Baveghems[a†], Ajith Pattammattel,[a‡] Monica E. Koubeck[a], Katharine Bruder[a], Challa V. Kumar[a,b,c]**

a. University of Connecticut, Department of Chemistry, U3060, Storrs, CT, USA, 06269
b. University of Connecticut, Department of Molecular and Cell Biology, Storrs, CT, USA, 06269
c. University of Connecticut, Institute of Materials Science, Storrs, CT USA, 06269

Experimental

CD Spectroscopy

A Jasco J-710 CD spectrophotometer (Easton, MD) with 0.02 cm path length quartz cuvettes, in the wavelength range of 260–200 nm was used. Bandwidth and the sensitivity were set to 1 nm and 50 millidegrees, respectively. Three scans were accumulated for each sample and the average spectrum was recorded. The samples were used directly after stirring and were diluted to micromolar concentrations. All spectra were normalized per micro molar bound enzyme per 1 cm path length and has been compared to the spectra of the corresponding unbound enzyme, measured under the same conditions.

Results and Discussion:

Standard curve to determine the concentration of exfoliated α-ZrP (mg/mL) from the absobance value at 350 nm

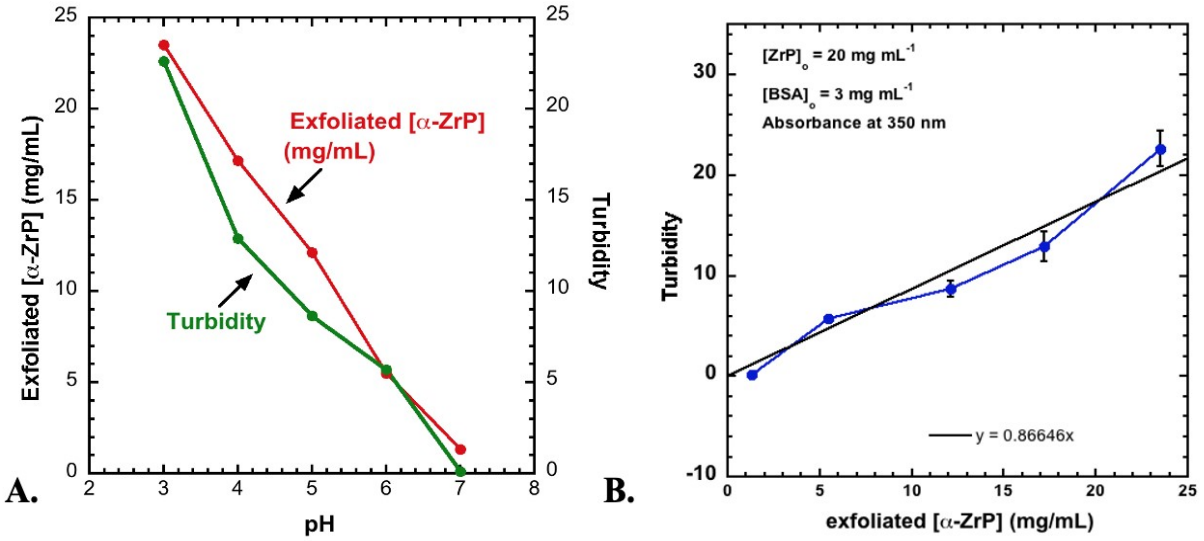

Figure S1: **A.** Concentration of exfoliated α-ZrP and turbidity (calculated as the product of absobance of the suspension at 350 nm and the dilution factor used) as a function of pH. **B.** Standard curve plotted by correlating turbidity and concentration of exfoliated α-ZrP (mg/mL) at different pH to calculate the concentration of exfoliated α-ZrP as a function of turbidity (or absorbance at 350 nm). The calculated extinction coefficient at 350 nm was 0.86646 L mol^{-1} cm^{-1}.

X-ray Powder Diffraction of exfoliated α-ZrP (mg/mL) at different exfoliation time (min)

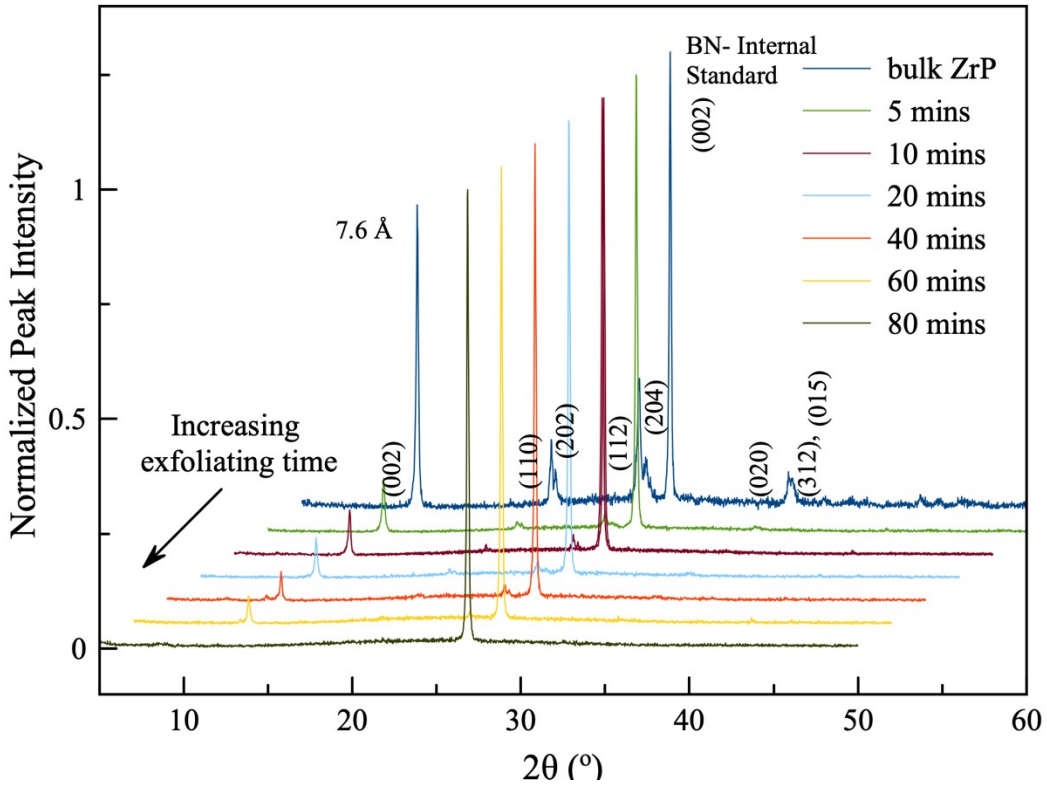

Figure S2: XRD diffractograms of exfoliated α-ZrP at different exfoliation time.

XRPD of exfoliated α-ZrP at different pH

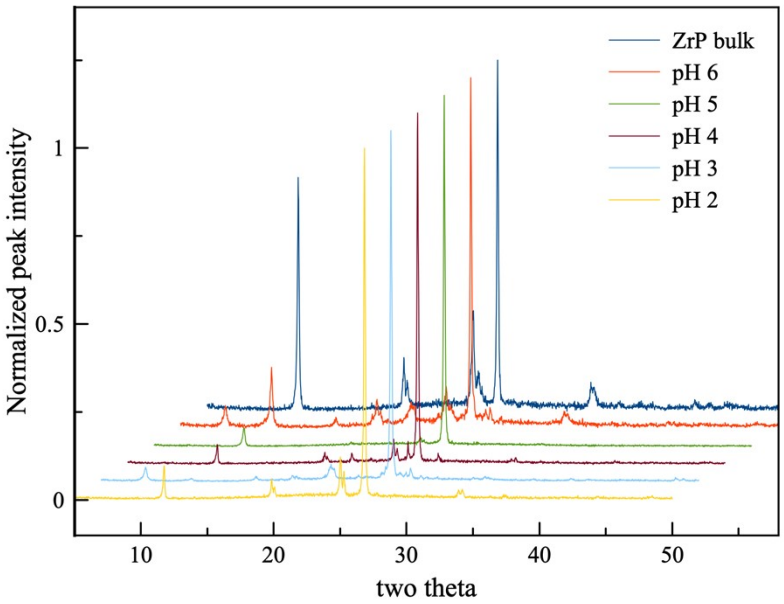

Figure S3: XRD patterns of exfoliated α-ZrP at different pH.

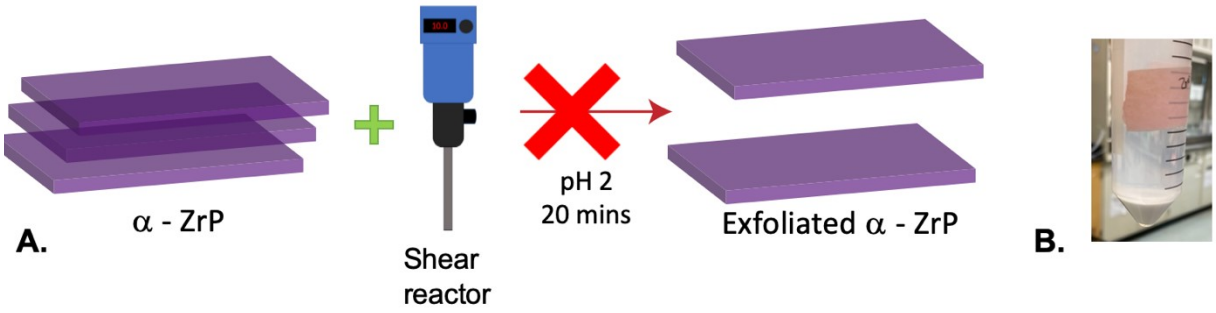

Figure S4: Exfoliation of α-ZrP at pH 2 without BSA. **A**. Schematic showing the procedure for exfoliating α-ZrP at pH 2 (10,000 rpm, 20 minutes shear time). **B**. the resultant dispersion displaying unsuccessful exfoliation (all sample precipitated at the bottom).

Microscopy of exfoliated α-ZrP:

SEM

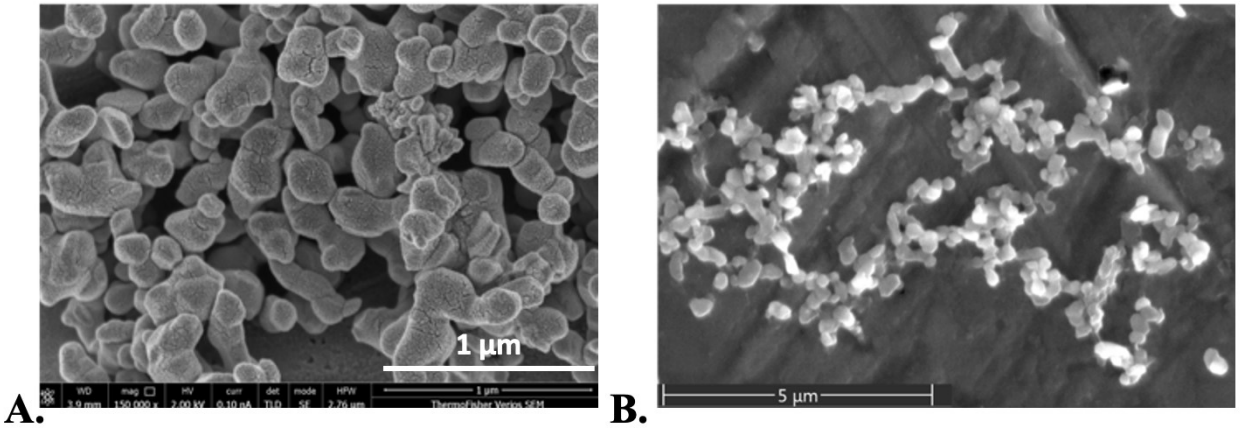

Figure S5: Electron microscopic images of bulk and exfoliated α-ZrP. SEM of **A**. unexfoliated α-ZrP **B**. exfoliated α-ZrP (unevenly coated by gold leading to different contrast).

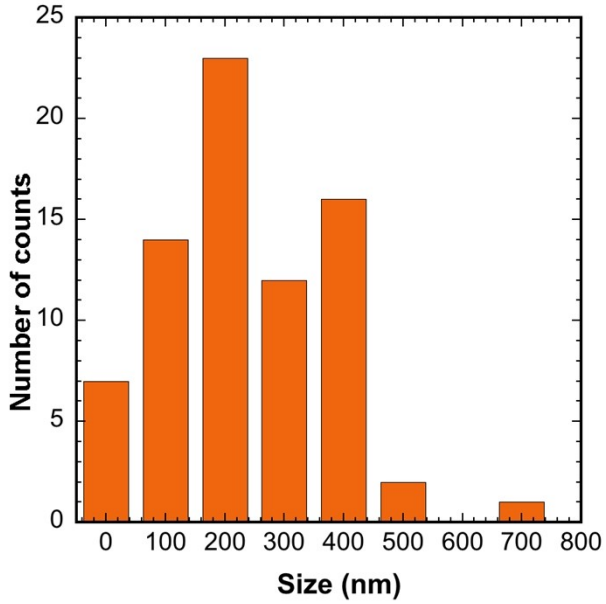

Figure S6: TEM Analysis for the exfoliated sample.

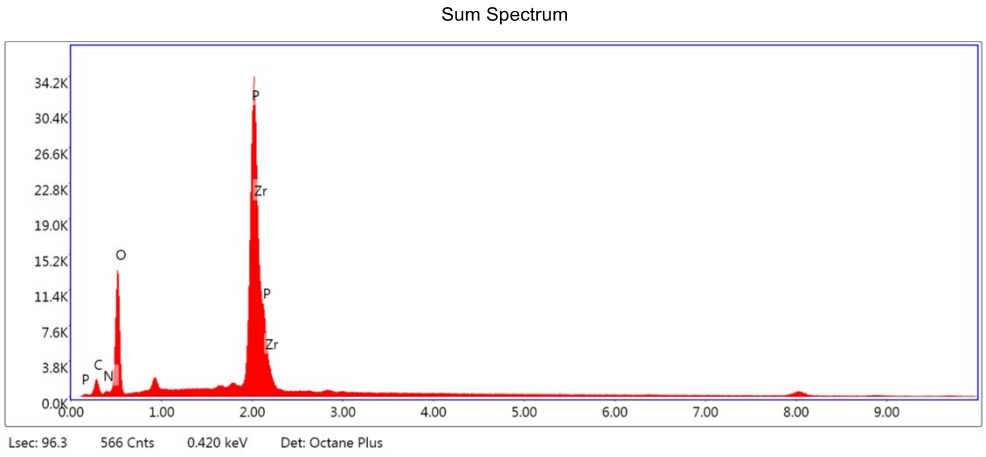

eZAF Smart Quant Results

Element	Weight %	Atomic %	Net Int.	Error %	Kratio	Z	A	F
C K	9.90	19.07	71.60	12.44	0.0156	1.1791	0.1334	1.0000
N K	3.38	5.59	24.40	15.14	0.0055	1.1513	0.1416	1.0000
O K	36.79	53.23	841.60	9.42	0.0905	1.1268	0.2183	1.0000
P K	19.13	14.30	1833.00	2.69	0.1702	0.9807	0.9007	1.0071
ZrL	30.80	7.82	1547.50	2.38	0.2535	0.7709	1.0681	0.9995

Figure S7: EDS sum spectrum of BSA exfoliated α-ZrP showing the peaks of elements detected as collected from SEM.

Correlation plot between initial concentration of BSA and BSA bound after the exfoliation process.

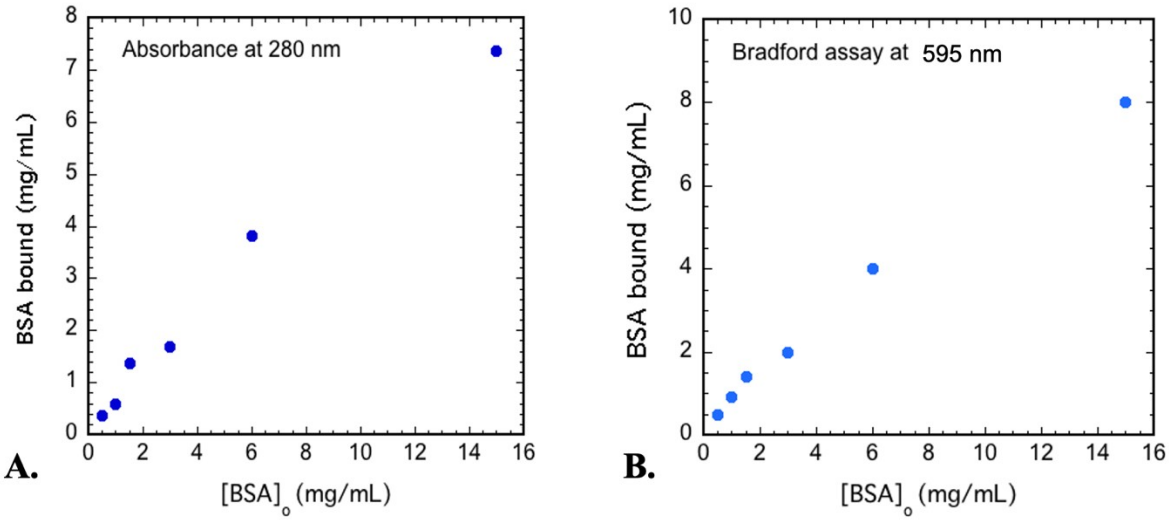

Figure S8: Correlation plot between the amount of BSA (mg/mL) added for exfoliation and BSA bound (mg/mL) to α-ZrP as calculated from **A.** absorbance measured 280 nm and **B**. Bradford assay absorbance at 595 nm.

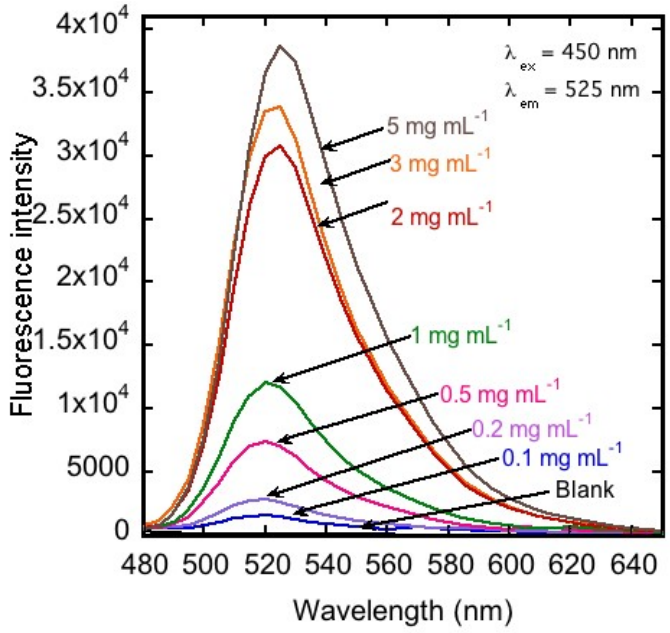

Figure S9: Standard curve to calculate the concentration of BSA from BSA-FITC fluorescence. The black curve represents the sodium phosphate buffer (20 mM, pH 7) used in studies

Exfoliation of ZrP with BSA-FITC via stirring method

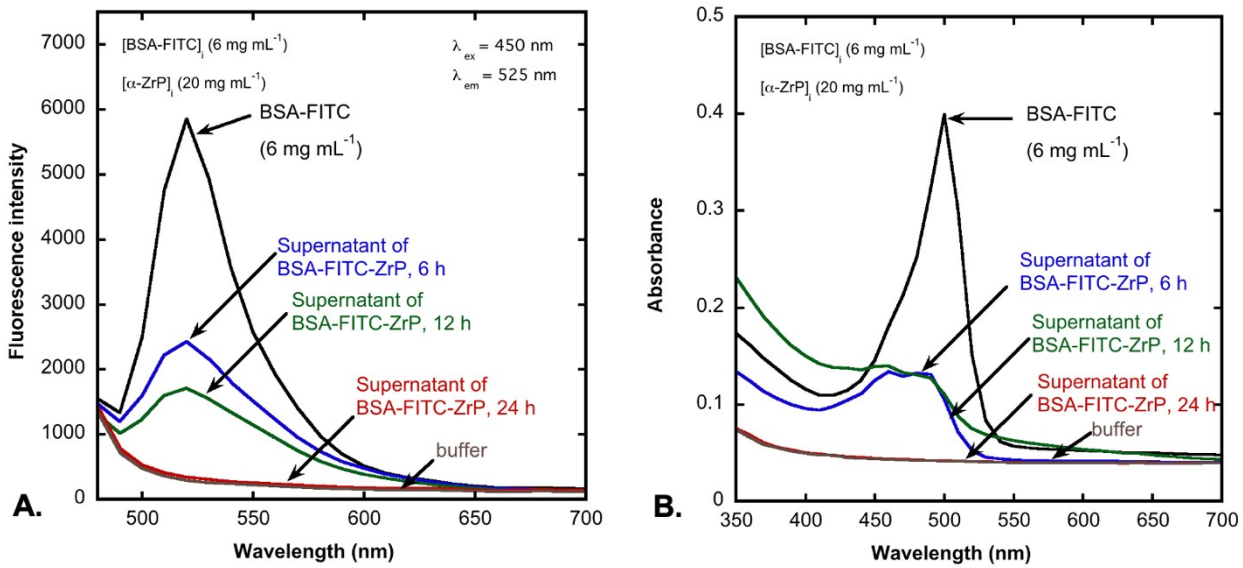

Figure S10 Time dependence of BSA-FITC depletion during exfoliation (A. Fluorescence and B. absorbance of the supernatant of BSA-FITC-ZrP samples at different times of stirring- Blue curve- 6 h, green curve- 12 h, red curve- 24 h)

Enzymology- Binding and Kinetics with stirring method

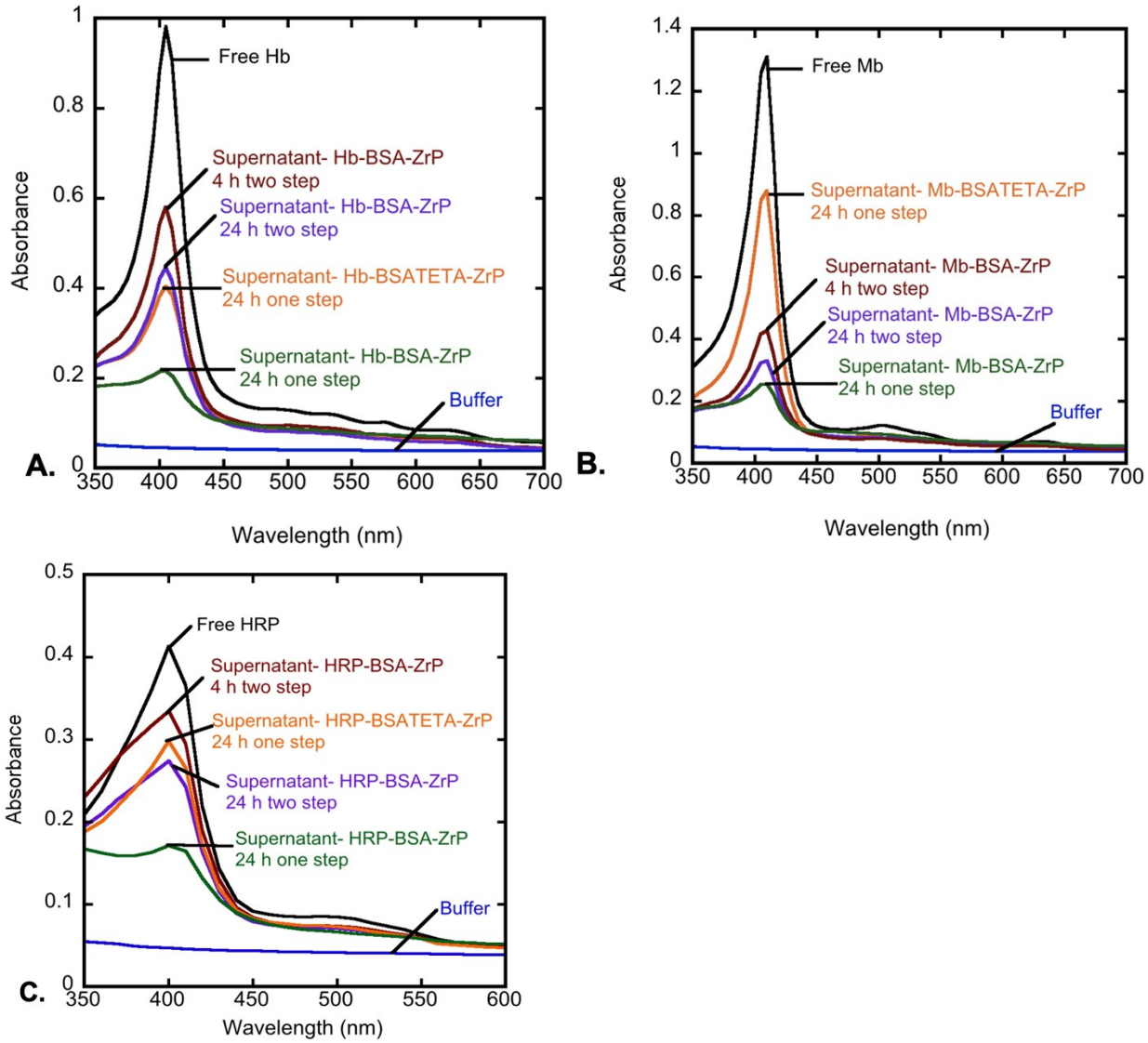

Figure S11: **Binding of enzymes in enzyme-BSA-ZrP samples (10 mM sodium phosphate buffer at pH 7) Absorbance spectra for supernatant of A. Hb-BSA-ZrP samples (depletion in peaks of Hb with respect to process followed) B. Mb-BSA-ZrP samples (depletion in peaks of Hb with respect to process followed) C. HRP-BSA-ZrP samples (depletion in peaks of HRP with respect to process followed).**

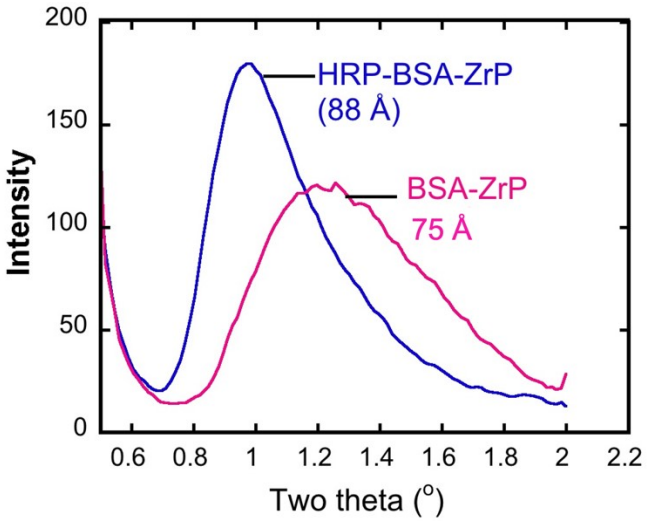

Figure S12: Small angle XRD showing proteins in the galleries of ZrP: HRP-BSA-ZrP (blue curve) and BSA-ZrP (pink curve) the corresponding d-spacing is shown in parentheses.

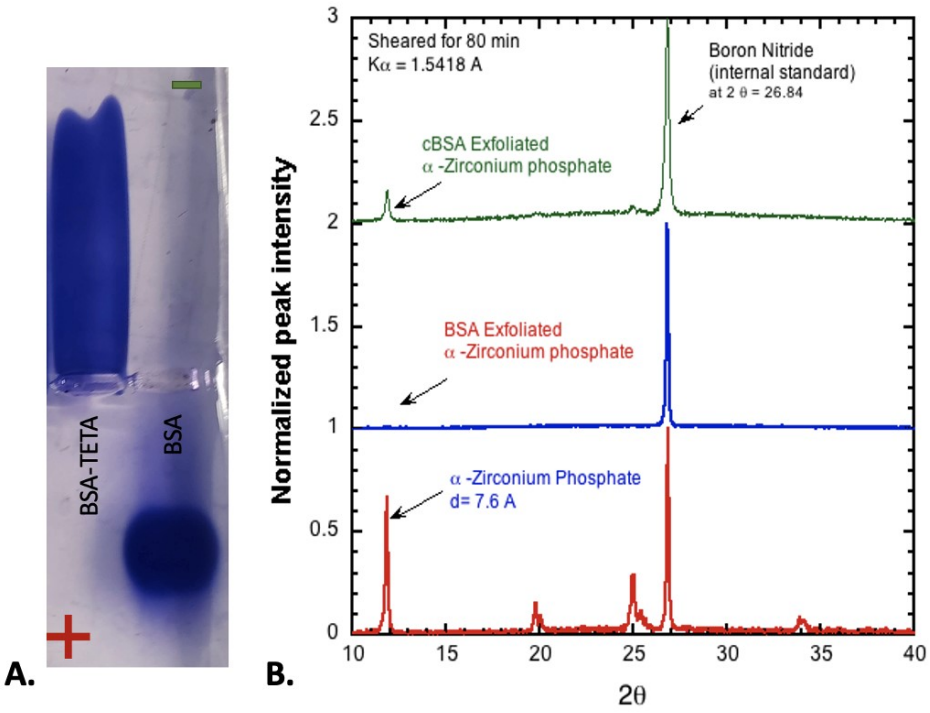

Figure S13: A. agarose gel showing cationized BSA (BSA midfied with TETA, charge +35). B.X-Ray Diffraction patterns of unexfoliated α-zirconium phosphate showing characteristic peak at d spacing = 7.6 Å and BSA and cBSA exfoliated α-Zirconium phosphate sheared at 80 minutes with no peak at d spacing = 7.6 Å (2θ = 11.84º). All XRD patterns were recorded with boron nitride as an internal standard and the characteristic BN peak at 2θ = 26.84º was used for

normalizing peak intensities. The exfoliation was performed under these conditions $[\alpha\text{-ZrP}]_0$ = 20 mg mL^{-1}, $[BSA]_0$ / $[BSA\text{-}TETA]_0$ = 3 mg mL^{-1} , pH 7.

Table S1: Amount of bound enzyme and the ratio of specific activity ratio of bound enzyme to the free enzymes

Sample	Parameters (Step, stirring time)	Specific activity ratio of bound to free enzyme	Bound enzyme (mg mL^{-1})
HRP-BSA-ZrP	Two step, 4 h	0.46 ± 0.02	0.2 ± 0.03
HRP-BSA-ZrP	Two step, 24 h	0.69 ± 0.04	0.33 ± 0.01
HRP-BSA-ZrP	One step, 24 h	0.60 ± 0.01	0.86 ± 0.02
HRP-BSA-TETA-ZrP	One step, 24 h	0.30 ± 0.02	0.35 ± 0.02
Mb-BSA-ZrP	Two step, 4 h	0.51 ± 0.04	0.32 ± 0.03
Mb-BSA-ZrP	Two step, 24 h	0.60 ± 0.05	0.53 ± 0.04
Mb-BSA-ZrP	One step, 24 h	0.84 ± 0.03	0.77 ± 0.06
Mb-BSA-TETA-ZrP	One step, 24 h	0.70 ± 0.04	0.30 ± 0.04
Hb-BSA-ZrP	Two step, 4 h	0.20 ± 0.05	0.41 ± 0.03
Hb-BSA-ZrP	Two step, 24 h	0.54 ± 0.02	0.51 ± 0.04
Hb-BSA-ZrP	One step, 24 h	0.55 ± .001	0.91 ± 0.02
Hb-BSA-TETA-ZrP	One step, 24 h	0.35± 0.003	0.610 ± 0.01

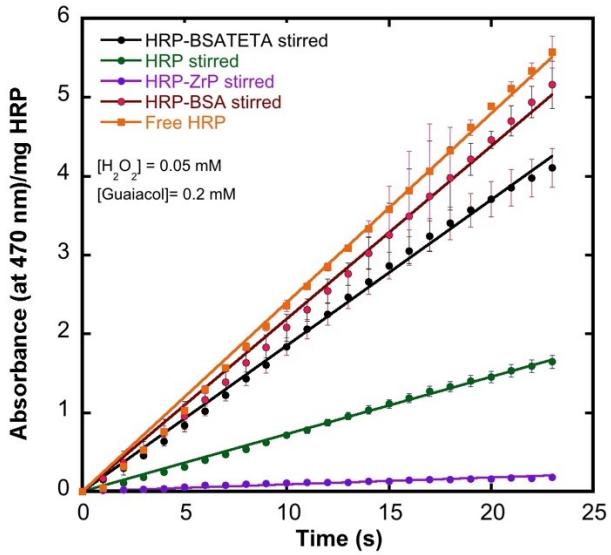

Figure S14: Stabilization of enzymes by BSA as observed from kinetics. Initial rate of peroxidase-like activity of free HRP (orange), HRP-BSA (red) stirred for 24 h, HRP-BSATETA (black) stirred for 24 h, HRP (green) stirred for 24 h, and HRP-ZrP stirred at 24 h, room temperature (10 mM sodium phosphate buffer at pH 7) by monitoring sample absorbance at 470 nm.

Table S2: Enzyme kinetics of stirred HRP (control sample). Specific activities and specific activity ratio of bound to free enzyme for HRP.

Sample	Parameters (Step, stirring time)	Specific activity (1µmol of substrate/min mg protein)	Specific activity ratio of bound to free enzyme
HRP free	-	6.3 ± 0.08	1
HRP stirred	- , 24 h	1.9 ± 0.05	0.31
HRP BSA stirred	- , 24 h	5.8 ± 0.08	0.93
HRP-BSATETA stirred	- , 24 h	4.9 ± 0.06	0.79
HRP-ZrP	One step, 24 h	2.3 ± 0.07	0.36

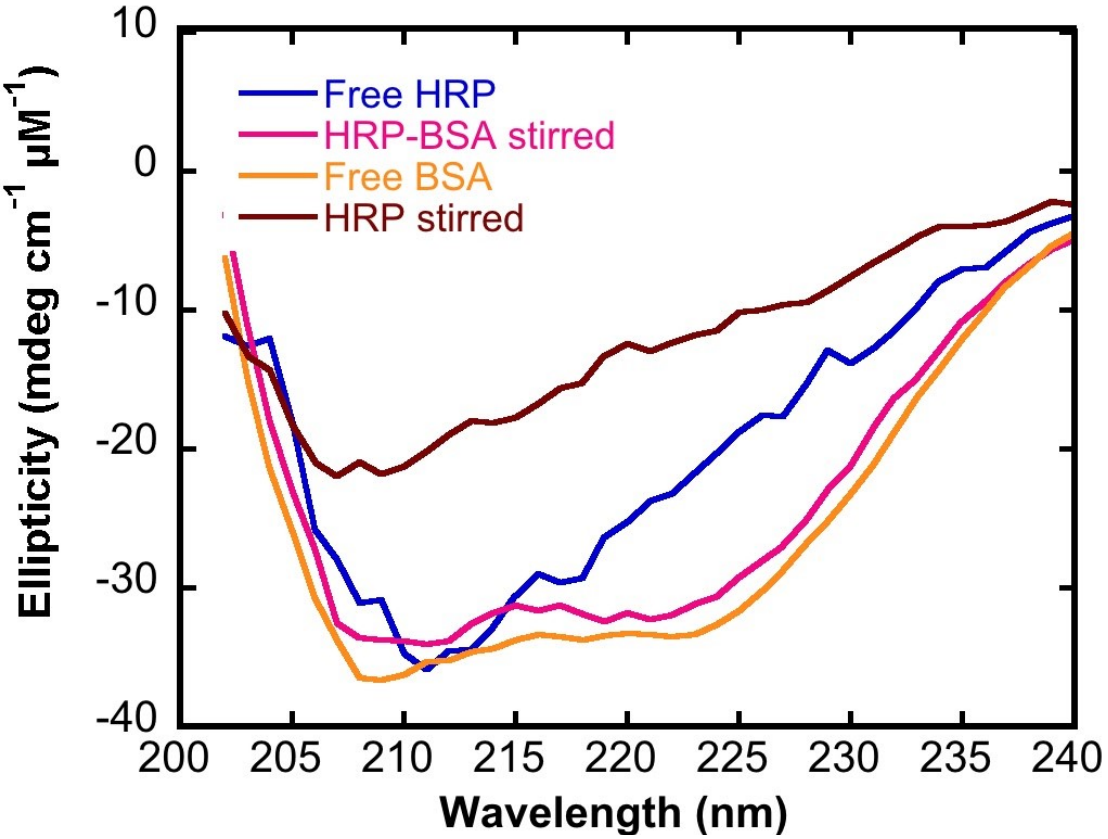

Figure S15: Effect of stirring on the structure of HRP. Far-UV CD spectra of Free HRP (blue, 100 µM HRP), HRP stirred for 24 h (dark brown, 10 µM HRP), HRP-BSA stirred for 24 h (pink, 36 µM, 0.6 mg/mL BSA, 10 µM, 0.1 mg/mL HRP- 6:1 :: BSA (mg) :HRP (mg)) and free BSA (orange, 36 µM, 0.6 mg/mL). Higher concentration of BSA dominates the CD of HRP which hence cannot be realized in Far-UV CD spectra.

Table S3: Specific activities of bound enzyme for one step and two step processes.

Sample	Parameters (Step, stirring time)	Specific activity (1µmol of substrate/min mg protein)
HRP-BSA-ZrP	Two step, 4 h	2.9 ± 0.1
HRP-BSA-ZrP	Two step, 24 h	4.9 ± 0.3
HRP-BSA-ZrP	One step, 24 h	3.8 ± 0.07
Free HRP	-	6.3± 0.08
HRP-BSA-TETA-ZrP	One step, 24 h	1.83 ± 1.2
Mb-BSA-ZrP	Two step, 4 h	0.05 ± 0.004
Mb-BSA-ZrP	Two step, 24 h	0.060 ± 0.005
Mb-BSA-ZrP	One step, 24 h	0.090 ± 0.003
Free Mb	-	0.1 ± 0.02
Mb-BSA-TETA-ZrP	One step, 24 h	0.80 ± 0.05
Hb-BSA-ZrP	Two step, 4 h	0.021 ± 0.005
Hb-BSA-ZrP	Two step, 24 h	0.055 ± 0.002
Hb-BSA-ZrP	One step, 24 h	0.056 ± .001
Free Hb	-	0.10 ± 0.03
Hb-BSA-TETA-ZrP	One step, 24 h	0.035 ± 0.003

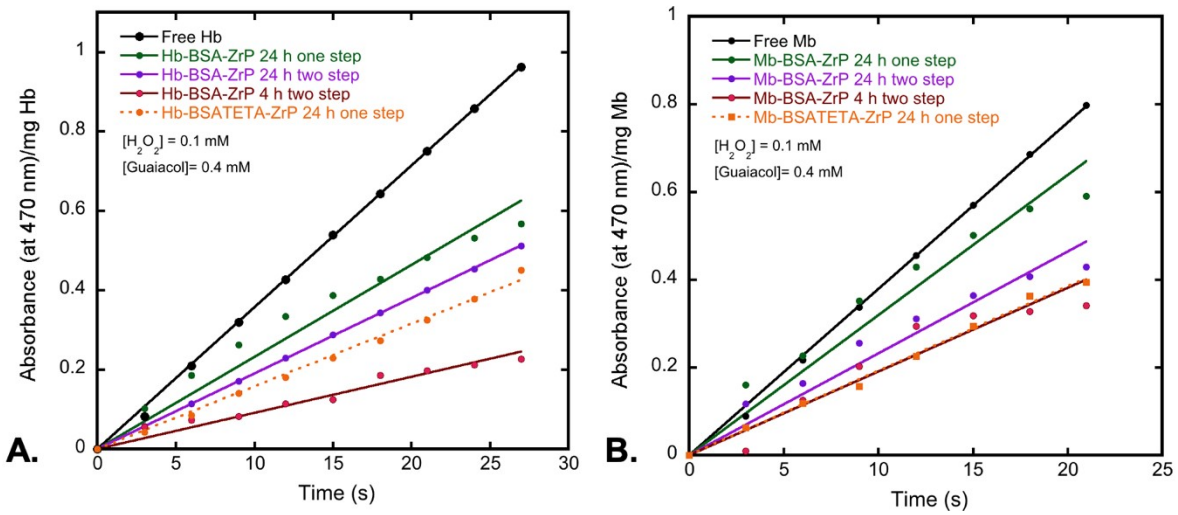

Figure S16: Enzyme kinetics of the bound enzymes. Initial rate of peroxidase-like activity of A. Hb B. Mb (10 mM sodium phosphate buffer at pH 7) by monitoring sample absorbance at 470 nm at room temperature.

Table S4: Dimensional comparison for bench stop stirrer (small volume) versus shear reactor (large volume).

Parameters	Bench top stirrer	Shear Reactor (IKA)	units
Diameter of beaker	1.5	2.4	cm
Radius of beaker (r)	0.75	1.2	cm
Height of Solution (h)	0.6	4.5	cm
Stir bar/shaft length	1.3	8.7	cm
stir bar/shaft height	0.2	27.1	cm
stir bar/shaft width	0.2	10.6	cm
Ratio of Beaker Diameter: Stir bar length	1.154	0.276	cm:cm
Ratio of Height of solution to height of stir bar	3	0.166	cm:cm
Volume expected ($\pi r^2 h$)	1.060	20.347	cm^3 or mL
Volume of exfoliated sample made	0.7	17	mL
Concentration achieved	10	10	mg/mL
Exfoliation Efficiency	7	170	mg
Shear rate	1000	10000	rpm
Shear time	24	0.33	h
Temperature	25	25	ºC

Order of rate results:

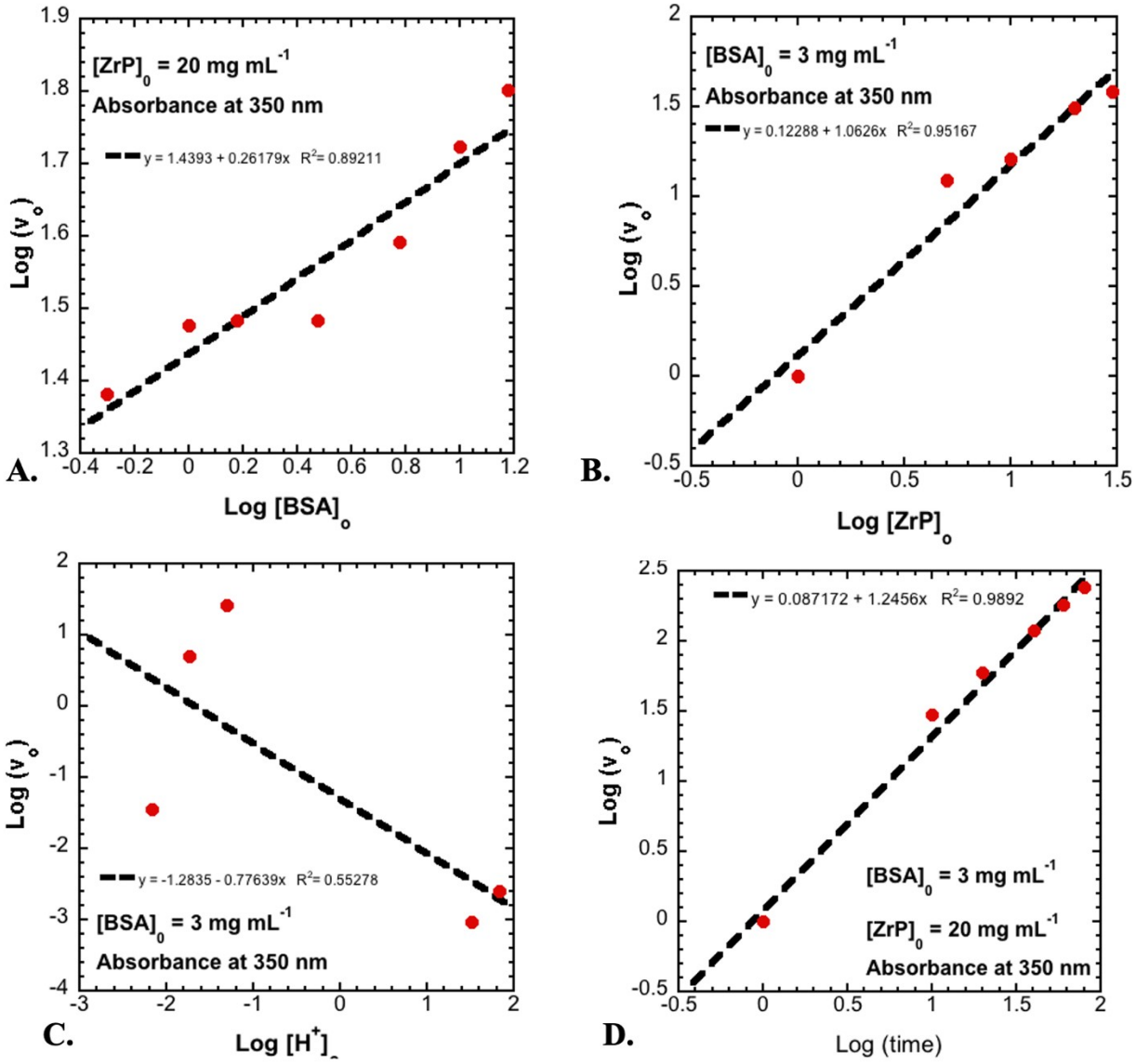

Figure S17: Log-log plots to determine the order of the reaction with respect to initial concentration of BSA ($[BSA]_0$) (**A**), initial concentration of α-ZrP ($[ZrP]_0$) (**B**), H^+ concentration (**C**), and time (**D**).

Correlation of different physical and chemical properties of proteins with percent peak intensity of exfoliated α-ZrP.

Table S5: Values for various properties of proteins (Part 1)

Protein	Charge at pH 7 (electrons)	diameter (nm)	total SASA/energy (Å²/Kcal/mol)*	Polar SASA/energy (Å²/Kcal/mol)*	Apolar SASA/energy (Å²/Kcal/mol)	molecular weight (kDa)
BSA	-27	7.3	28683.69	20713.09	37794.19	66.4
hemoglobin	-6	6.9	24548.47	7558.11	16990.35	64.5
β-lactoglobulin	-18	5.5	14708.87	5894.97	8814.3	18.3
ovalbumin	-38	5.4	54224.67	19987.47	34237.19	42.7
glucose oxidase	-30	8.6	20479.66	8833.76	11645.9	160
lysozyme	8	1.8	8686.49	2659.13	3636.7	14.7

* the values were calculated using Getarea software, available for free online.[1]

Table S6: Values for various properties of proteins (Part 2)

Proteins	Pdb id	Hydrophobic Residues (nonpolar)	Hydrophilic Residues (polar)	# of Arginine on each chain	# of Lysine on each chain	# of residues /protein	Viscosity (cPa)
BSA	4f5s[2]	232	351	23	59	583	40[3]
Hemoglobin	1a3n[4]	308	266	12	44	574	5.8[5]
β-lactoglobulin	1beb[6]	144	176	3	15	320	2.14[7]
Ovalbumin	1ova[8]	755	809	15	20	1564	25[9]
Glucose oxidase	1cf3[10]	287	296	22	15	583	24[11]
Lysozyme	1dpx[12]	75	89	11	6	164	15[13]

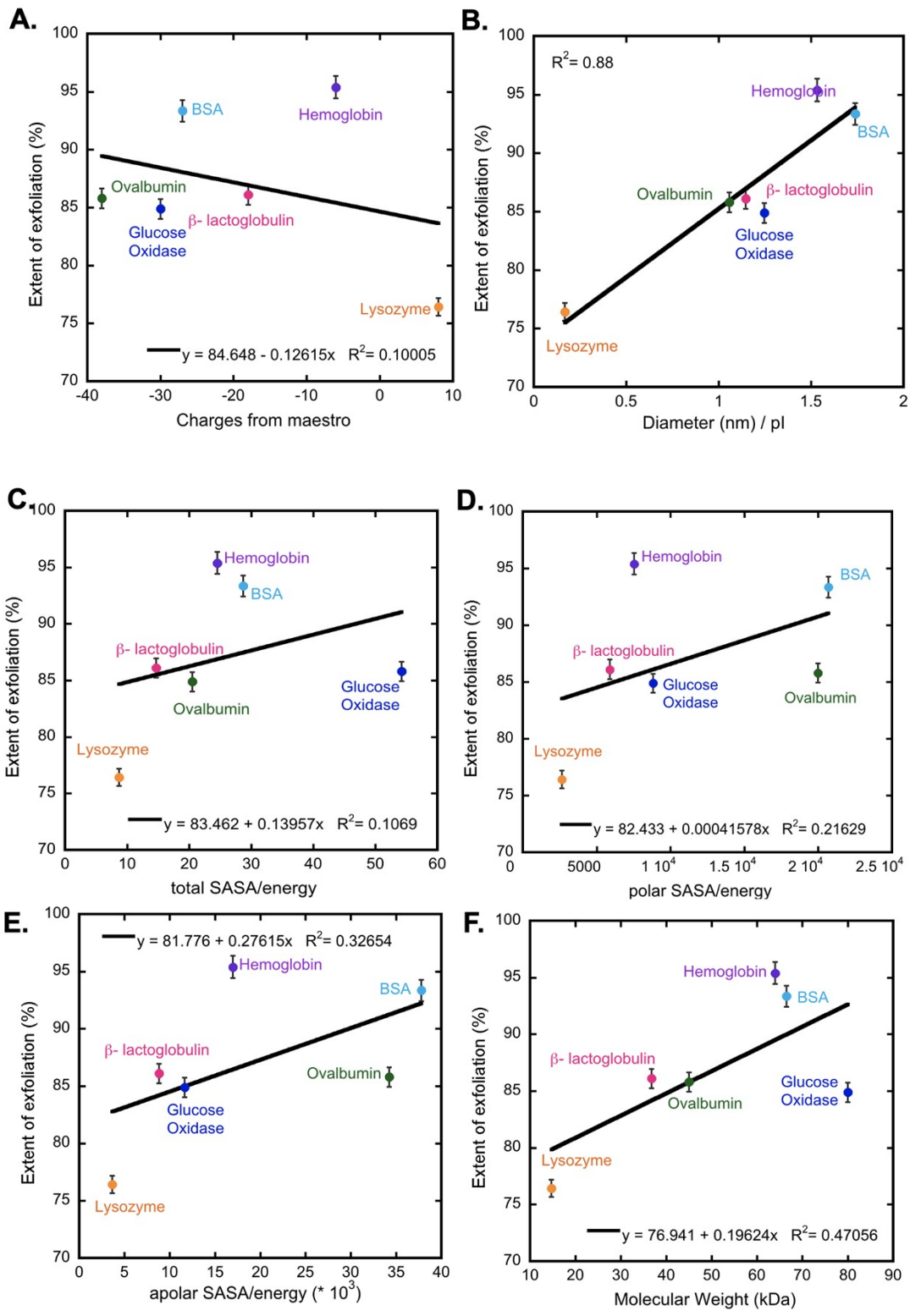
A.
Extent of exfoliation (%)
Charges from maestro
BSA
Hemoglobin
Ovalbumin
β- lactoglobulin
Glucose Oxidase
Lysozyme
y = 84.648 - 0.12615x R²= 0.10005
B.
R²= 0.88
Diameter (nm) / pI
C.
total SASA/energy
y = 83.462 + 0.13957x R²= 0.1069
D.
polar SASA/energy
y = 82.433 + 0.00041578x R²= 0.21629
E.
apolar SASA/energy (* 10³)
y = 81.776 + 0.27615x R²= 0.32654
F.
Molecular Weight (kDa)
y = 76.941 + 0.19624x R²= 0.47056

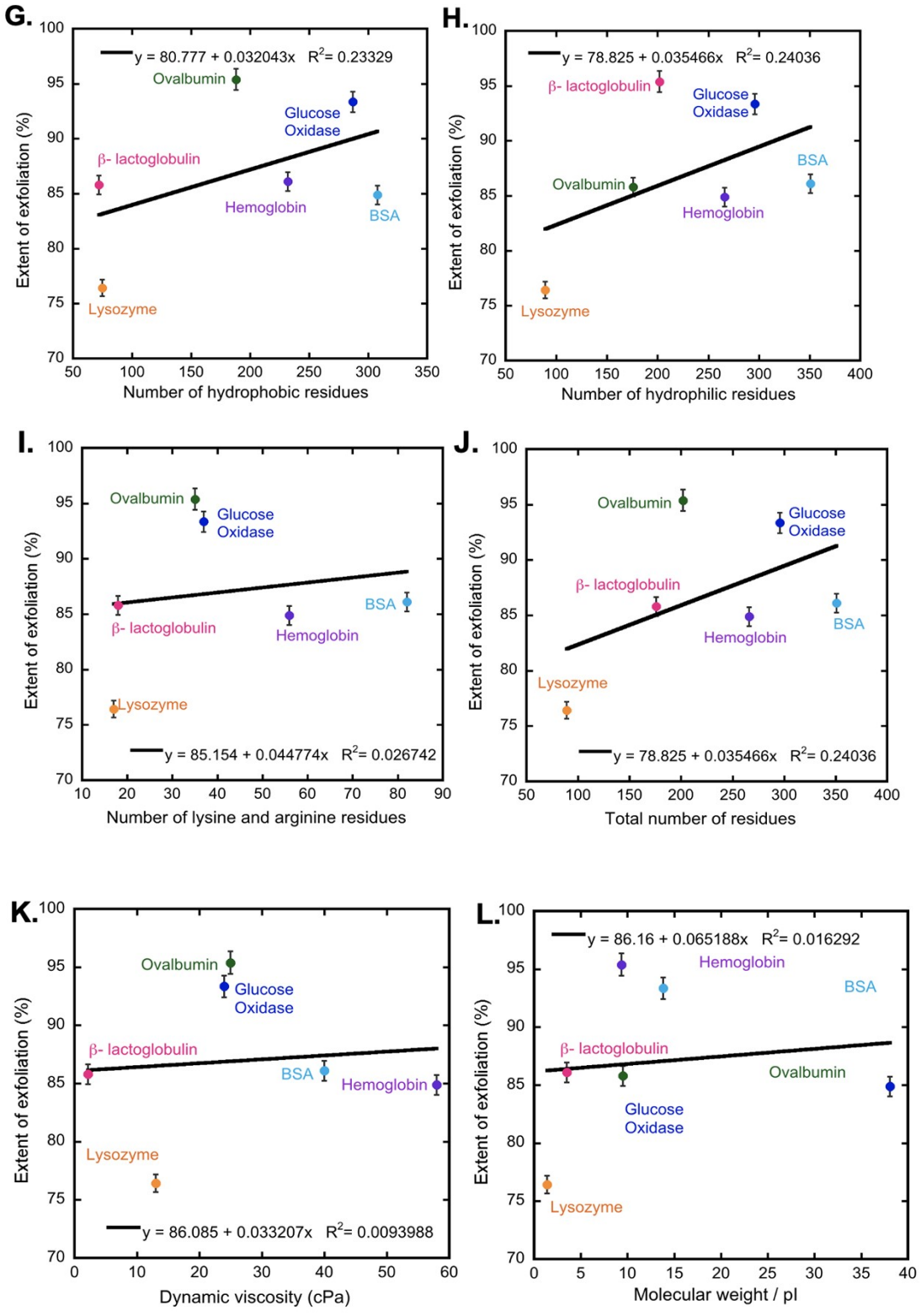

Figure S18: Percent peak intensity at 7. 6 Å plotted against **A.** charge at pH 5 of the protein as calculated by maestro, Schrödinger suites **B.** Diameter (nm)/pI of the protein **C.** Total

SASA/energy of the protein **D**. Polar SASA/energy of the protein **E.** Apolar SASA/energy of the protein as calculated by GetArea software* **F.** molecular weight of the protein **G.** Number of hydrophobic residues in the protein **H.** Number of hydrophilic residues in the protein **I.** Number of lysine and arginine residues in the protein **J.** Total number of residues in the protein in the protein **K.** Dynamic viscosity (cPa) of the protein **L.** molecular weight/ pI of the protein .

* (http://curie.utmb.edu/getarea.html)

References:

1 Fraczkiewicz, R., Braun, W. Exact and Efficient Analytical Calculation of the Accessible Surface Areas and Their Gradients for Macromolecules. *J. Comp. Chem.*, **1998**, ***19***, 319-333.

2 Bujacz, A., Structures of bovine, equine and leporine serum albumin. *Acta crystallographica. Section D, Biological crystallography* **2012,** *68* (Pt 10), 1278-89.

3 Lin, J.-L.; Chu, M.-L.; Chen, C.-H., A portable multiple ionization source biological mass spectrometer. *Analyst* **2020**.

4 Tame, J. R.; Vallone, B., The structures of deoxy human haemoglobin and the mutant Hb Tyralpha42His at 120 K. *Acta crystallographica. Section D, Biological crystallography* **2000,** *56* (Pt 7), 805-11.

5 Heidema, A. G.; Nagelkerke, N., Developing a Discrimination Rule between Breast Cancer Patients and Controls Using Proteomics Mass Spectrometric Data: A Three-Step Approach. **2008,** *7* (2).

6 Brownlow, S.; Morais Cabral, J. H.; Cooper, R.; Flower, D. R.; Yewdall, S. J.; Polikarpov, I.; North, A. C.; Sawyer, L., Bovine beta-lactoglobulin at 1.8 A resolution--still an enigmatic lipocalin. *Structure (London, England : 1993)* **1997,** *5* (4), 481-95.

7 Richert, Manuela E.; Gochev, Georgi G.; Braunschweig, Björn, Specific Ion Effects of Trivalent Cations on the Structure and Charging State of β-Lactoglobulin Adsorption Layers. *Langmuir.* Aug **2019.** 35, 11299-11307

8 Stein, P. E.; Leslie, A. G.; Finch, J. T.; Carrell, R. W., Crystal structure of uncleaved ovalbumin at 1.95 A resolution. *Journal of molecular biology* **1991,** *221* (3), 941-59.

9 Watanabe, E.; Tsoka, S.; Asenjo, J.A., Selection of Chromatographic Protein Purification Operations Based on Physicochemical Properties. *Annals of the New York Academy of Sciences.* June **1994**. *721*(1), 348-364.

10 Wohlfahrt, G.; Witt, S.; Hendle, J.; Schomburg, D.; Kalisz, H. M.; Hecht, H. J., 1.8 and 1.9 A resolution structures of the Penicillium amagasakiense and Aspergillus niger glucose oxidases as a basis for modelling substrate complexes. *Acta crystallographica. Section D, Biological crystallography* **1999,** *55* (Pt 5), 969-77.

11 Zhao, K.; Gu, W.; Zheng, S.; Zhang, C.; Xian, Y., SDS–MoS2 nanoparticles as highly-efficient peroxidase mimetics for colorimetric detection of H2O2 and glucose. *Talanta* **2015,** *141*, 47-52.

12 Weiss, M. S.; Palm, G. J.; Hilgenfeld, R., Crystallization, structure solution and refinement of hen egg-white lysozyme at pH 8.0 in the presence of MPD. *Acta crystallographica. Section D, Biological crystallography* **2000,** *56* (Pt 8), 952-8.

13 Ladam, G.; Schaaf, P.; Decher, G.; Voegel, J; Cuisinier, F.J., Protein adsorption onto auto-assembled polyelectrolyte films. *Biomolecular Engineering.* Aug **2002.** *19*(2-6), 273-280.